11th World Congress on Structural and Multidisciplinary Optimisation
07th -12th, June 2015, Sydney Australia

Reliability-Based Design Optimization of Wind Turbine Blades for Fatigue Life under Wind Load Uncertainty

Weifei Hu[1], K.K. Choi[1], Hyunkyoo Cho[1], Nicholas J. Gaul[1], Olesya I. Zhupanska[1]

[1] The University of Iowa, Iowa City, Iowa, USA, kyung-choi@uiowa.edu

1. Abstract

Conventional wind turbine blades have been designed using fatigue life predictions based on a fixed wind load distribution that does not fully capture uncertainty of the wind load. This could result in early fatigue failure of blades and eventually increase the maintenance cost of wind turbines. To produce reliable as well as economical wind turbine blades, this paper studies reliability-based design optimization (RBDO) of a wind turbine blade using a novel wind load uncertainty model. In the wind load uncertainty model, annual wind load variation has been extended over a large spatiotemporal range using 249 groups of wind data. The probability of fatigue failure during 20-year service life is estimated using the uncertainty model in the RBDO process and is reduced to meet a desired target probability of failure. Meanwhile, the cost of composite materials used in the blade is minimized by optimizing the composite laminate thicknesses of the blade. In order to obtain the RBDO optimum design efficiently, deterministic design optimization (DDO) of a 5-MW wind turbine blade is first carried out using the mean wind load obtained from the uncertainty model. At the DDO optimum design, fatigue hotspots for RBDO are identified among the laminate section points. For efficient sampling-based RBDO process to handle dynamic wind load uncertainty, instead of generating surrogate models of the overall output performance measure, which is 20-year fatigue life, a number of surrogate models of the 10-minute fatigue damages D_{10} at the hotspots are accurately created using the dynamic Kriging (DKG) method. Using these surrogate models and the wind load uncertainty model, probability of failure of 20-year fatigue life at these hotspots and their design sensitivities are calculated at given design points. Using the sampling-based method, RBDO of the 5-MW wind turbine blade is carried out starting at the DDO optimum design to meet the target probability of failure of 2.275%.

2. Keywords: Wind Turbine Blade, Reliability-Based Design Optimization, Fatigue Life, Wind Load Uncertainty

3. Introduction

As an expensive component in large wind turbine systems, designing reliable wind turbine blades for 20-year fatigue life is one of the most important factor in wind turbine design. A cost-effective design of the blades reduces the initial investment, and a reliable design reduces maintenance cost of the wind turbine systems. This paper proposes reliability-based design optimization (RBDO) process and methods for optimizing reliable wind turbine blades considering dynamic wind load uncertainty.

It is challenging to accurately predict the fatigue damage/life of wind turbine blades due to various uncertainties from material properties, manufacturing process, and external loads. Among those uncertainties, dynamic wind load uncertainty is the most significant source of uncertainty affecting the fatigue reliability of wind turbine blades. Hence, better understanding of the dynamic wind load uncertainty is critical for the reliable optimum design of wind turbine blades.

Reliability analysis of wind turbine blades considering wind load uncertainty has been studied [1-6]. Probabilistic models for mean wind speed have been applied to characterize the annual wind load variation [1-10]. Measured fatigue loadings, e.g., stress and bending moment, were applied to wind turbine fatigue and reliability analysis [3,4]. Traditional reliability analysis of wind turbines involves a specific distribution, e.g., Weibull distribution or Rayleigh distribution, of mean wind speed to account for the frequency of fatigue damage under different wind loads. However, by applying a fixed Weibull distribution, only deterministic fatigue life can be obtained because the assumed Weibull distribution is invariant in different years. The fixed Weibull distribution based either on wind turbine standards [11,12] or measured wind data over one year at a specific location cannot truly render the wind load uncertainty over a larger spatiotemporal range, for instance at different locations and in different years. Tarp-Johansen [5] has studied the statistical uncertainty of two parameters of the Weibull distribution for mean wind speed based on one-year measurements over a period of 52 years.

Besides the mean wind speed, the fluctuations in the wind speed about the short-term mean naturally have a significant impact on the design loadings, as they are the source of extreme gust loads and a large part of the blade fatigue loading [13,14]. The distribution of turbulence intensity has been involved in the reliability analysis of wind turbine blades [1,6]. Another simple way to consider the wind load uncertainty is by using partial safety factors [11,12,15-17]. However, the spatial and temporal wind load variation cannot be represented accurately

using partial safety factors. In this paper, the reliability analysis of wind turbine blades applies a wind load uncertainty model, which considers both annual wind load variation and wind load variation in a large spatiotemporal range.

Reliability-based design of wind turbine blades against fatigue failure has been studied by Ronold et al. [1], whose probabilistic model was applied to reliability analysis of a site-specific wind turbine of a prescribed make. Toft and Sørensen [18] presented a probabilistic framework for design of wind turbine blades, which requires tests with the basic composite materials and full-scale blades during the design process. Reliability-based design of wind turbines against failure under extreme condition has also been studied [19,20]. However, very few research has well addressed RBDO of wind turbine blades for fatigue life under wind load uncertainty. This paper presents RBDO of wind turbine blades for fatigue life using the developed wind load uncertainty model, by which the obtained RBDO optimum design satisfies a reliability requirement considering realistic uncertain wind load during the designed 20-year lifespan.

4. Fatigue Analysis of Composite Wind Turbine Blades

4.1. Parametric blade modelling

A parametric composite wind turbine blade model has been developed for fatigue analysis, deterministic design optimization (DDO), reliability analysis and RBDO. The aerodynamic properties of the blade model, e.g., airfoil type, chord length, and twist angle, are the same with the 5-MW NREL reference wind turbine blade [21]. However, material properties and laminate schedules are different from the NREL blade. The current blade is composed of seven parts, which are the root, forward shear web, aft shear web, leading edge, spar cap, trailing edge, and tip, as shown in Fig. 1. Each part consists of a different number of panels. In total, there are 71 panels in the seven parts. The forward shear web, aft shear web, leading edge, and trailing edge consist of sandwich panels, in which composite laminates are laid at both the top and bottom surfaces and a foam core is laid in the middle. Other parts are made of composite laminates. Composite laminates QQ1 and P2B are selected from the SNL/MSU/DOE Composite Material Fatigue Database [22]. The laminate thicknesses of QQ1 and P2B in panels are changing in DDO and RBDO because they are connected to the design variables for DDO and RBDO.

4.2. Fatigue analysis procedure

A comprehensive fatigue analysis procedure has been developed to calculate 10-minute fatigue damage D_{10} given blade design variable vector $\mathbf{d}$, 10-minute mean wind speed V_{10}, and 10-minute turbulence intensity I_{10}. The design variable vector $\mathbf{d}$ controls the thicknesses of composite laminates used in the wind turbine blade. The fatigue analysis procedure is briefly explained as follows.

Given the V_{10} and I_{10} at hub height, a 10-minute wind field realization is first simulated using TurbSim [23]. The simulated wind field is then used to calculate resultant aerodynamic lift force, drag force, and moment force at the aerodynamic centre of each blade section by AeroDyn [24]. In order to avoid stress concentration using resultant aerodynamic forces, detailed wind pressure obtained from XFOIL [25] is modified to match the aerodynamic forces calculated by AeroDyn. Then, the modified wind pressure could be applied on the blade surface to carry out FEA using Abaqus [26]. Detailed explanation of obtaining the modified wind pressure is provided in the previous work [27]. At the same time, gravity load and centrifugal load have been considered in the stress analysis. The non-proportional multi-axial complex stresses at section points, which indicate locations through laminate thickness in the wind turbine blade, is extracted out for fatigue damage calculation. A multi-axial fatigue damage index [28] is used to calculate the fatigue damage considering longitudinal stress σ_{11}, transverse stress σ_{22}, and shear stress σ_{12} in principal material coordinates. The 95% lower bounds of the probabilistic S-N curves and constant life diagrams (CLDs) are applied when calculating the number of allowable cycles at a certain stress level. Finally, the 10-minute fatigue damage at a section point is accumulated by Miner's rule.

In summary, the 10-minute fatigue damage D_{10} at a section point in the blade can be determined by design variable vector $\mathbf{d}$, 10-minute mean wind speed V_{10}, and 10-minute turbulence intensity I_{10} as

$$D_{10} = D_{10}\left(\mathbf{d}, V_{10}, I_{10}\right) \tag{1}$$

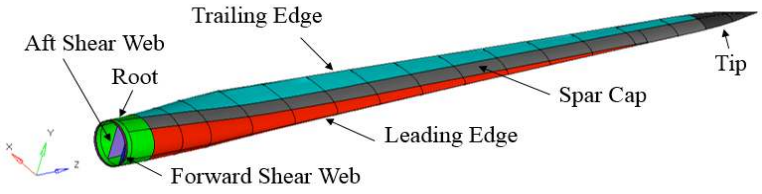

Figure 1: Seven Parts of the Composite Wind Turbine Blade

5. Dynamic Wind Load Uncertainty Model

The developed wind load uncertainty model involves both the annual wind load variation and the wind load variation in a large spatiotemporal range. The annual wind load variation represents variation of 10-minute mean wind speed V_{10} and 10-minute turbulence intensity I_{10} in a year using a joint probability density function (PDF) of V_{10} and I_{10}. However, it is not appropriate to obtain the joint PDF of V_{10} and I_{10} directly from their marginal PDFs due to the correlation between V_{10} and I_{10}. It is found that V_{10} and I_{10} have statistical correlation. Moreover, there is also a mathematical correlation between V_{10} and I_{10} because I_{10} is calculated by Σ_{10}/V_{10}, where Σ_{10} is 10-minute standard deviation of wind speed. To exclude the mathematical correlation in the joint PDF, the joint PDF of V_{10} and Σ_{10} is obtained first and then transferred to the joint PDF of V_{10} and I_{10}.

Based on the 249 groups of wind data, the marginal PDFs of V_{10} and Σ_{10} have been identified to be Weibull distribution and Gamma distribution, respectively, using the Maximum Likelihood Estimate (MLE) method [29]. The statistical correlation between V_{10} and Σ_{10} is represented using Gumbel copula, which is also the maximum likely copula type [30]. Because the transformation from the random vector (V_{10}, Σ_{10}) to the random vector (V_{10}, I_{10}) is a one-to-one transformation with the Jacobian of the transformation $J = v_{10}$, the joint PDF of V_{10} and I_{10} could be derived using the joint PDF of V_{10} and Σ_{10} as

$$f_{VI}\left(v_{10},i_{10}\right)=f_{V\Sigma}\left(v_{10},\sigma_{10}\right)\left|J\right|=f_{V\Sigma}\left(v_{10},v_{10}\cdot i_{10}\right)v_{10} \tag{2}$$

where f_{VI} and $f_{V\Sigma}$ are the joint PDFs for (V_{10}, I_{10}) and (V_{10}, Σ_{10}), respectively; v_{10}, i_{10} and σ_{10} are realizations of V_{10}, I_{10}, and Σ_{10}, respectively; and $\sigma_{10} = v_{10} \cdot i_{10}$. Using the identified copula for V_{10} and Σ_{10}, the joint PDF of V_{10} and Σ_{10} can be expressed as [30]

$$f_{V\Sigma}\left(v_{10},\sigma_{10}\right)=c_{V\Sigma}\left(v_{10},\sigma_{10}\right)f_{V10}\left(v_{10}\right)f_{\Sigma10}\left(\sigma_{10}\right) \tag{3}$$

where $c_{V\Sigma}$ is the copula density function for V_{10} and Σ_{10}, and f_{V10} and $f_{\Sigma10}$ are the marginal PDFs of V_{10} and Σ_{10}, respectively. Using Eqs. (2) and (3), the joint PDF of V_{10} and I_{10} can be expressed as

$$f_{VI}\left(v_{10},i_{10}\right)=c_{V\Sigma}\left(v_{10},v_{10}\cdot i_{10}\right)f_{V10}\left(v_{10}\right)f_{\Sigma10}\left(v_{10}\cdot i_{10}\right)v_{10} \tag{4}$$

The marginal PDFs of Weibull distribution for V_{10} and Gamma distribution for Σ_{10} take the forms

$$f_{V10}\left(v_{10};C,k\right)=\frac{k}{C}\left(\frac{v_{10}}{C}\right)^{k-1}\exp\left[-\left(\frac{v_{10}}{C}\right)^{k}\right] \tag{5}$$

$$f_{\Sigma10}\left(\sigma_{10};a,b\right)=\frac{1}{b^{a}\Gamma\left(a\right)}\sigma_{10}^{a-1}\exp\left(-\frac{\sigma_{10}}{b}\right) \tag{6}$$

respectively, where C and k are the scale parameter and shape parameter for the Weibull distribution, respectively; a and b are the shape parameter and scale parameter for the Gamma distribution, respectively; and $\Gamma(a)$ is the gamma function of a. The Gumbel copula density function $c_{V\Sigma}$ for V_{10} and Σ_{10} is expressed as [30]

$$c_{V\Sigma}\left(u,v;\theta\right)=\frac{\left(-\ln u\right)^{\theta-1}\left(-\ln v\right)^{\theta-1}\left(\theta+w^{1/\theta}-1\right)w^{1/\theta-2}\exp\left(-w^{1/\theta}\right)}{uv} \tag{7}$$

where u and v are marginal cumulative distribution functions (CDFs) of V_{10} and Σ_{10}, respectively; w is equal to $\left(-\ln u\right)^{\theta}+\left(-\ln v\right)^{\theta}$; and θ is the copula parameter, which can be calculated from Kendall's tau τ as [30]

$$\theta=1/\left(1-\tau\right) \tag{8}$$

Based on Eqs. (4) - (8), the derived joint PDF of V_{10} and I_{10} is determined by parameters C, k, a, b, and τ. Using the 249 groups of wind data, 249 different sets of (C, k, a, b, τ) have been calculated. Each set of (C, k, a, b, τ) contains annual wind load variation. The calculated 249 sets of (C, k, a, b, τ) indicate that there is a wind load variation in the large spatiotemporal range, i.e., in different years and at different locations. Therefore, the dynamic wind load variation in the large spatiotemporal range can be represented by providing the distributions of (C, k, a, b, τ). These distributions are identified by the MLE method using the 249 sets of (C, k, a, b, τ). The identified distribution types of C, k, a, b, and τ are log-logistic, normal, generalized extreme value, Weibull, and extreme value distributions, respectively. The specific parameters for PDFs of C, k, a, b, and τ are obtained as well from the 249 sets, assuming that C, k, a, b, and τ are statistically independent. Due to space limitations, these PDFs are omitted from presentation here.

6. Reliability Analysis under Dynamic Wind Load Uncertainty

6.1. Twenty-year Fatigue Damage Calculation

Applying the 10-minute fatigue damage D_{10} in Eq. (1) and the derived joint PDF of V_{10} and I_{10} in Eq. (4), the one-year fatigue damage D_{1year} can be calculated as

$$D_{1year}\left(\mathbf{d},C,k,a,b,\tau\right)=52560\int_{V_{low}}^{V_{upp}}\int_{I_{low}}^{I_{upp}}f_{VI}\left(v_{10},i_{10};C,k,a,b,\tau\right)D_{10}\left(\mathbf{d},v_{10},i_{10}\right)\mathrm{d}v_{10}\mathrm{d}i_{10} \tag{9}$$

where "52560" indicates the number of 10-minute periods in one year; V_{low} and V_{upp} are the lower and upper bounds of V_{10}, respectively; and I_{low} and I_{upp} are the lower and upper bounds of I_{10}, respectively. The one-year fatigue damage in Eq. (9) cannot be explicitly expressed as a function of **d**, C, k, a, b, and τ, due to the complexity of the joint PDF and 10-minute fatigue damage calculation. Thus, in practical damage calculation, the double integration in Eq. (9) is numerically calculated using the Riemann integral as

$$D_{1year}\left(\mathbf{d},C,k,a,b,\tau\right)\approx 52560\sum_{i=1}^{m}\sum_{j=1}^{n}P_{VI}^{i,j}\left(v_{10}^{i},i_{10}^{j};C,k,a,b,\tau\right)D_{10}^{i,j}\left(\mathbf{d},v_{10}^{i},i_{10}^{j}\right) \tag{10}$$

where m and n are the number of selected V_{10} and I_{10}, respectively. The probability of the V_{10} and I_{10} in (i,j) cell can be calculated as

$$P_{VI}^{i,j}\left(v_{10}^{i},i_{10}^{j};C,k,a,b,\tau\right)=f_{VI}\left(v_{10}^{i},i_{10}^{j};C,k,a,b,\tau\right)\Delta v_{10}\Delta i_{10} \tag{11}$$

where Δv_{10} and Δi_{10} are the size of the (i,j) cell in directions of V_{10} and I_{10}, respectively. (v_{10}^{i}, i_{10}^{j}) is the center point of the (i, j) cell. In this paper, a large range of V_{10} and I_{10} has been considered to examine the fatigue damage considering all possible wind conditions, i.e., combination of V_{10} and I_{10}. The lower bound and upper bound of V_{10} are set to be the cut-in wind speed of 3 m/s and cut-out wind speed of 25 m/s, respectively [21]. The lower bound and upper bound of I_{10} are set to be 0.02 and 1, respectively. The 10-minute fatigue analyses are run over the range of V_{10} between 3 m/s and 25 m/s in 2 m/s increments, and the range of I_{10} between 0.02 and 1 in 0.02 increments. Therefore, the number of realizations of V_{10} and I_{10} are m = 12 (i =1,…,12) and n = 50 (j =1,…,50), respectively, in Eq. (10). At each wind condition, a wind load probability $P_{VI}^{i,j}$ is calculated using Eq. (11), and a 10-minute fatigue damage $D_{10}^{i,j}$ is calculated using the developed fatigue analysis procedure in Section 4.2. In this way, a 12-by-50 wind load probability table for $P_{VI}^{i,j}$ and a 12-by-50 10-minute fatigue damage table for $D_{10}^{i,j}$ can be constructed.

Considering the wind load variation in a 20-year range, a 20-year fatigue damage at a given design **d** can be calculated as

$$\begin{aligned}D_{20year}\left(\mathbf{d},\mathbf{C},\mathbf{k},\mathbf{a},\mathbf{b},\boldsymbol{\tau}\right)&=\sum_{t=1}^{20}D_{1year}^{t}\left(\mathbf{d},C^{t},k^{t},a^{t},b^{t},\tau^{t}\right)\\&=52560\sum_{t=1}^{20}\sum_{i=1}^{12}\sum_{j=1}^{50}P_{VI}^{i,j}\left(v_{10}^{i},i_{10}^{j};C^{t},k^{t},a^{t},b^{t},\tau^{t}\right)D_{10}^{i,j}\left(\mathbf{d},v_{10}^{i},i_{10}^{j}\right)\end{aligned} \tag{12}$$

where random vectors **C**, **k**, **a**, **b**, and **τ** contain 20 sets of (C, k, a, b, τ) as $\mathbf{C}=[C^1, C^2,\ldots, C^{20}]$, $\mathbf{k}=[k^1, k^2,\ldots, k^{20}]$, $\mathbf{a}=[a^1, a^2,\ldots, a^{20}]$, $\mathbf{b}=[b^1, b^2,\ldots, b^{20}]$, and $\boldsymbol{\tau}=[\tau^1, \tau^2,\ldots, \tau^{20}]$. The realizations of random vectors can be randomly drawn from the obtained PDFs of C, k, a, b, and τ in Section 5.

6.2. Reliability Analysis Using Monte Carlo Simulation

In this paper, the probability of fatigue failure is calculated using a sampling-based reliability method that uses Monte Carlo simulation (MCS). Using Eq. (12) and MCS, the probability of fatigue failure is calculated as

$$\begin{aligned}P\left(\text{Fatigue Life } < \text{ 20 years}\right)&=P\left(D_{20year}\left(\mathbf{Y}\right)>1\right)=\int_{D_{20year}(\mathbf{Y})>1}f_{\mathbf{Y}}\left(\mathbf{y}\right)d\mathbf{y}\\&=\int_{N}I_{\Omega_F}\left(\mathbf{y}\right)f_{\mathbf{Y}}\left(\mathbf{y}\right)d\mathbf{y}\cong\frac{1}{NMCS}\sum_{i=1}^{NMCS}I_{\Omega_F}\left[\mathbf{y}^{(i)}\right]\end{aligned} \tag{13}$$

where $\mathbf{Y}=[\mathbf{X}, \mathbf{C}, \mathbf{k}, \mathbf{a}, \mathbf{b}, \boldsymbol{\tau}]$, and $\mathbf{y}^{(i)}$ is the i^{th} realization of $\mathbf{Y}$. It is worth noting that the realization $\mathbf{y}^{(i)}$ is randomly generated based on the PDF of a random design vector **X** and the PDFs of random parameters (C, k, a, b, τ) in the wind load uncertainty model. In reliability analysis, the realizations of **X** replace the design variable vector **d** in order to consider the design uncertainty. The mean of the random design vector **X** is the design variable vector **d** in RBDO. Each realization $\mathbf{y}^{(i)}$ includes 20 sets of (C, k, a, b, τ), which represent the wind load variation in 20 years. $NMCS$ is the number of realizations for MCS. Ω_F is the failure domain such that $D_{20year}(\mathbf{Y}) > 1$, and I_{Ω_F} is an

indicator function defined as

$$I_{\Omega_F}(\mathbf{y}) = \begin{cases} 1, & \text{for } \mathbf{y} \in \Omega_F \\ 0, & \text{otherwise} \end{cases} \tag{14}$$

7. Reliability-Based Design Optimization under Dynamic Wind Load Uncertainty

7.1. Random Design Variables

In RBDO, the uncertainty of composite laminate thickness due to the manufacturing process has been considered. The coefficient of variation (CoV) of thicknesses of QQ1 and P2B laminate are referred from the SNL/MSU/DOE Composite Material Fatigue Database [22]. There are seven random design variables that control laminate thicknesses in seven parts accordingly. A linear relationship is used to link an RBDO design variable to laminate thicknesses in panels of a part. The linear relationship between each RBDO design variable and the linked laminate thicknesses is based on the DDO optimum design, as the normalized DDO optimum design variables are used as the initial design variables of RBDO. Due to space limitations, the DDO procedure and results are omitted in this paper. The properties of random design variables for RBDO are listed in Table 1, where $\mathbf{d}^L$, $\mathbf{d}^O$, and $\mathbf{d}^U$ are the normalized lower bound, mean, and upper bound of the random design variables, respectively. The CoV of a random design variable is equal to that of thickness of the corresponding composite laminate and is fixed in the RBDO process.

Table 1: Properties of Random Design Variables

Random Design Variable	Distribution	$\mathbf{d}^L$	$\mathbf{d}^O$	$\mathbf{d}^U$	CoV	Corresponding Part	Composite Laminate
d_1	Normal	0.7811	1	3.1243	0.0323	Root	QQ1
d_2	Normal	0.6820	1	2.2741	0.0323	Forward Shear Web	QQ1
d_3	Normal	1.0000	1	1.9133	0.0323	Aft Shear Web	QQ1
d_4	Normal	0.6014	1	2.4057	0.0323	Tip	QQ1
d_5	Normal	0.8974	1	3.5897	0.0323	Leading Edge	QQ1
d_6	Normal	0.4823	1	1.9291	0.0323	Trailing Edge	QQ1
d_7	Normal	0.4626	1	1.3878	0.0203	Spar Cap	P2B

7.2. Objective Function

The normalized total cost of composite materials that are used in the blade is set as the objective function, which is expressed as

$$C(\mathbf{d}) = \left(4.18 \times 1000 \times \sum_{i}^{6} m_i^0 \frac{d_i}{d_i^0} + 11.70 \times 1000 \times m_7^0 \frac{d_7}{d_7^0} \right) \Big/ Cost^0 \tag{15}$$

where m_i^0 (unit: ton) is the initial mass of the i^{th} part; d_i^0 is the normalized initial design variable corresponding to the i^{th} part; normalized d_i is the current design corresponding to the i^{th} part; i= 1, 2, …, 7; and $Cost^0$ is the initial cost. According to TPI Composites, the material costs of QQ1 and P2B are taken to be \$4.18/kg and \$11.70/kg, respectively [31]. It is worth noting that the cost of the carbon/glass-hybrid-fiber-reinforced laminate P2B is 2.799 times more expensive than that of QQ1, which is a glass-fiber-reinforced laminate. The objective function in Eq. (15) is minimized in the RBDO process.

7.3. Probabilistic Constraints

The probabilistic constraint is that the probability of fatigue failure in Eq. (13) at a hotspot should be smaller than a target probability of failure P_F^{tar}=2.275%. Hotspots are the section points in seven parts (corresponding to seven design variables) that show maximum fatigue damage at the RBDO initial design. For the current RBDO problem, there are seven probabilistic constraints corresponding to seven hotspots, which are identified at the DDO optimum design. The probabilistic constraints are expressed as

$$P\left(D_{20\,year}^j(\mathbf{Y}) > 1\right) \le P_{F_j}^{\text{tar}} = 2.275\%, \quad j = 1, \ldots, 7 \tag{16}$$

In order to efficiently calculate 20-year fatigue damage in Eq. (12), accurate global surrogate models for 10-minute fatigue damage D_{10} with respect to design variables have been created using the dynamic Kriging (DKG) method [32]. Because each RBDO constraint requires 600 D_{10}'s corresponding to 12-by-50 different wind conditions (see Section 6.1), there are 4,200 D_{10} surrogate models for seven RBDO constraints. The design of

experiments (DoE) samples for creating surrogate models are sequentially sampled. In total, 1,000 DoE samples are used for creating all 4,200 D_{10} surrogate models. After the accurate surrogate models are created, the design sensitivities of the probabilistic constraints are calculated using MCS and score function [33].

The ratio between true 20-year fatigue damage using the 10-minute fatigue analysis procedure and predicted 20-year fatigue damage using D_{10} surrogate models is calculated. The same MCS of 20 sets of (C, k, a, b, τ) are used for the two types of 20-year fatigue damage. The ratios are calculated at another 1000 design points randomly drawn in the design domain. Table 2 shows the minimum ratio, mean ratio, maximum ratio, standard deviation of ratios, and number of ratios between 0.99 and 1.01 among 1000 ratios for each RBDO constraint. Because the numbers of ratios between 0.99 and 1.01 are larger than 950 (95%), the surrogate models are treated as accurate surrogate models for RBDO.

Table 2: Accuracy Check for Surrogate Models

RBDO Constraint	Minimum Ratio	Mean Ratio	Maximum Ratio	Standard Deviation of Ratios	Number of Ratios Between 0.99 and 1.01
1	0.9939	1.0001	1.0099	0.0013	1000
2	0.9850	1.0002	1.0137	0.0030	990
3	0.9617	1.0001	1.0480	0.0051	963
4	0.9929	0.9998	1.0083	0.0019	1000
5	0.9851	0.9999	1.0260	0.0048	957
6	0.9771	0.9998	1.0347	0.0049	957
7	0.9638	1.0002	1.0276	0.0030	994

7.4. RBDO Formulation and Procedure

The RBDO problem can be formulated as

$$\begin{aligned} &\text{minimize} && \text{Cost}(\mathbf{d}) \\ &\text{subject to} && P\left(D^{j}_{20\,year}\left(\mathbf{Y}\right)>1\right) \le P^{\text{tar}}_{F_j} = 2.275\%, \quad j=1,\ldots,7 \\ & && \mathbf{d}^{L} \le \mathbf{d} \le \mathbf{d}^{U}, \quad \mathbf{d} \in \quad ^{7} \text{ and } \mathbf{X} \in \quad ^{107} \end{aligned} \tag{17}$$

where $\mathbf{Y}$ is the 107-dimensional random vector including seven random design variables and 20 sets of (C, k, a, b, τ); $\mathbf{d}$ is the 7-dimensional design variable vector; Cost($\mathbf{d}$) is the normalized cost as shown in Eq. (15); and $D^{j}_{20\,year}$ is the 20-year fatigue damage for the j^{th} probabilistic constraint $P\left(D^{j}_{20\,year}\left(\mathbf{Y}\right)>1\right) \le P^{\text{tar}}_{F_j}$. The flowchart of the RBDO procedure including global surrogate model generation is given in Fig. 2.

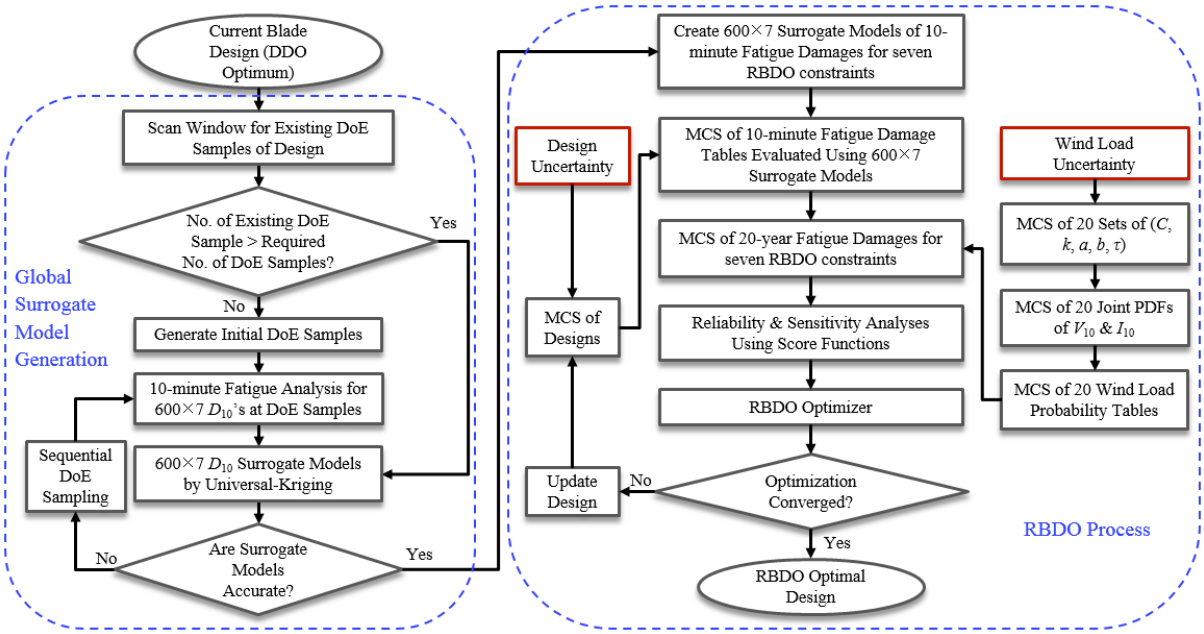

Figure 2: Flowchart of the RBDO Procedure Including Global Surrogate Model Generation

8. Results and Discussion

The RBDO procedure is successfully converged using 13 iterations. At each iteration, 200,000 MCS of 20 sets of (C, k, a, b, τ) are used to calculate the probabilities of failure and design sensitivities of the probabilistic constraints. The probability of failure was reduced from 56.902% at the RBDO initial design (DDO optimum design) to 2.369% at the RBDO optimum design. The histories of the normalized cost and maximum probability of failure among seven RBDO constraints are shown in Figure 3. Table 3 compares the RBDO initial design, RBDO optimum design, true cost, and weight. It is observed that through the RBDO process the cost is reduced by 8% while the weight is increased by 13.3%. The reason is that more cheap but heavy composite material, QQ1, is applied at the RBDO optimum design than that applied at the RBDO initial design. Meanwhile, a less expensive composite material, P2B, is chosen at the RBDO optimum design.

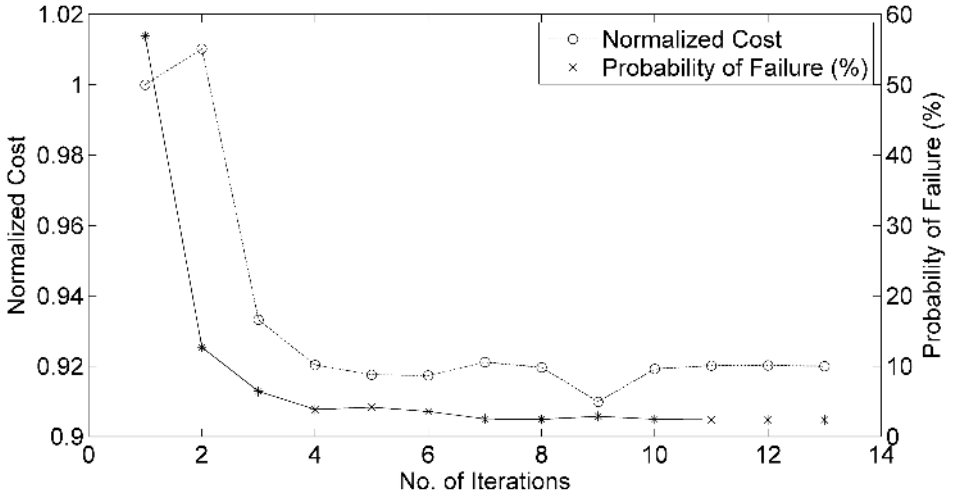

Figure 3: Histories of the Normalized Cost and Maximum Probability of Failure among Seven RBDO Constraints

Table 3: Comparison of the RBDO Initial Design and RBDO Optimum Design

	d_1	d_2	d_3	d_4	d_5	d_6	d_7	Cost ($)	Weight (ton)
RBDO Initial Design	1	1	1	1	1	1	1	101331	17.7473
RBDO Optimum Design	1.1885	2.1922	1.9132	0.6987	0.9968	1.3262	0.5413	93224	20.1080

9. Conclusions

The RBDO of wind turbine blades for fatigue life under wind load uncertainty is investigated in this paper. The wind load uncertainty model could provide realistic uncertain wind load through the designed 20-year lifespan. A reliability analysis method for wind turbine blades under the wind load uncertainty model has been developed. Based on the reliability analysis method, RBDO has been carried out to obtain fatigue reliable design for a 20-year lifespan considering wind load uncertainty. The obtained RBDO optimum design minimizes the material cost and reduces the probability of failure to 2.369% based on the current surrogate models. This research demonstrates that applying RBDO methods to wind turbine blades could provide safer and more economical designs considering wind load uncertainty.

10. Acknowledgements

This research is primarily supported by the Iowa Alliance Wind Innovation and Novel Development (IAWIND) 09-IPF-15 and NSF EPSCoR project EPS-1101284. These supports are greatly appreciated.

11. References

[1] K.O. Ronold, W.H. Jakob and C.J. Christensen, Reliability-based fatigue design of wind-turbine rotor blades, *Engineering Structures*, 21 (12), 1101-1114, 1999.

[2] K.O. Ronold and C.J. Christensen, Optimization of a design code for wind-turbine rotor blades in fatigue, *Engineering Structures*, 23 (8), 993-1004, 2001.

[3] P.S. Veers and S.R. Winterstein, Application of measured loads to wind turbine fatigue and reliability

analysis, *Proceedings of 1997 ASME Wind Energy Symposium*, *35th AIAA Aerospace Science Meeting & Exhibit*, Reno, NV, 1997.
[4] J.H. Sutherland and P.S. Veers, Fatigue Case Study and Reliability analyses for Wind Turbines, *ASME/JSME/JSES International Solar Energy Conference*, Sandia National Laboratory, Albuquerque, 1995.
[5] N.J. Tarp-Johansen, Examples of Fatigue Lifetime and Reliability Evaluation of Larger Wind Turbine Components, Report No.: Risø-R-1418(EN), Risø National Laboratory, Denmark, 2003.
[6] W. Hu, K.K. Choi, N.J. Gaul, H. Cho and O. Zhupanska, Reliability Analysis of Wind Turbine Blades for Fatigue Life Under Wind Load Uncertainty, *14th AIAA/ISSMO Multidisciplinary Analysis and Optimization Conference*, Indianapolis, Indiana, September 17-19, 2012.
[7] D.T. Griffith and T.D. Ashwill, The Sandia 100-meter All-glass Baseline Wind Turbine Blade: SNL 100-00, SANDIA REPORT SAND2011-3779, Sandia National Laboratories, USA, 2011.
[8] J.A. Carta, P. Ramirez and S. Velazquez, A Review of Wind Speed Probability Distributions Used in Wind Energy Analysis Case Studies in the Canary Islands, *Renewable and Sustainable Energy Reviews*, 13 (5), 933-955, 2009.
[9] M.M. Shokrieh and R. Rafiee, Simulation of Fatigue Failure in A Full Composite Wind Turbine Blade, *Composite Structures*, 74, 332-342, 2006.
[10] L. Manuel, P.S. Veers and S.R. Winterstein, Parametric Models for Estimating Wind Turbine Fatigue Loads for Design, *Proceedings of 2001 ASME Wind Energy Symposium, 39th AIAA Aerospace Sciences Meeting & Exhibit*, Reno, NV, 2001.
[11] IEC 61400-1, Wind Turbines − Part I: Design Requirements, 3rd Ed., International Electrotechnical Commission, 2005.
[12] Germanischer Lloyd, Guideline for the Certification of Wind Turbines Edition 2010, Hamburg, Germany, 2010.
[13] T. Burton, N. Jenkins, D. Sharpe and E. Bossanyi, *Wind Energy Handbook, 2nd Ed.*, John Wiley & Sons, Ltd., West Sussex, UK, 2011.
[14] J.F. Manwell, J.G. Mcgowan and A. L. Rogers, *Wind Energy Explained: Theory, Design and Application 2nd Ed.*, John Wiley & Sons, Ltd., West Sussex, UK, 2009.
[15] C. Kong, J. Bang and Y. Sugiyama, Structural Investigation of Composite Wind Turbine Blade Considering Various Load Cases and Fatigue Life, *Energy*, 30, 2101-2114, 2005.
[16] C. Kong, T. Kim, D. Han and Y. Sugiyama, Investigation of Fatigue Life for A Medium Scale Composite Wind Turbine Blade, *International Journal of Fatigue*, 28, 1382-1388, 2006.
[17] D. Veldkamp, A Probabilistic Evaluation of Wind Turbine Fatigue Design Rules, *Wind Energy*, 11, 655-672, 2008.
[18] H.S. Toft and J.D. Sørensen, Reliability-based design of wind turbine blades, *Structural Safety*, 33 (6), 333-342, 2011.
[19] K.O. Ronold and G.C. Larsen, Reliability-based design of wind-turbine rotor blades against failure in ultimate loading, *Engineering Structures*, 22 (6), 565-574, 2000.
[20] P.W. Cheng, A Reliability Based Design Methodology for Extreme Responses of Offshore Wind Turbines, Ph.D. dissertation, Wind Energy Research Institute, Delft University of Technology, Netherlands, 2002.
[21] J. Jonkman, S. Butterfield, W. Musial and G. Scott, Definition of a 5-MW Reference Wind Turbine for Offshore System Development, NREL/TP-500-38060, Golden, CO, National Renewable Energy Laboratory, 2009.
[22] J.F. Mandell and D.D. Samborsky, SNL/MSU/DOE Composite Material Fatigue Database Mechanical Properties of Composite Materials for Wind Turbine Blades Version 23.0, Montana State University – Bozeman, 2014.
[23] B.J. Jonkman, TurbSim User's Guide: Version 1.50, NREL/TP-500-46198, Golden, CO, National Renewable Energy Laboratory, 2009.
[24] P. J. Moriarty and A.C. Hansen, AeroDyn Theory Manual, NREL/EL-500-3881, Golden, CO, National Renewable Energy Laboratory, 2005.
[25] M. Drela and H. Youngren, XFOIL 6.9 User Guide, Massachusetts Institute of Technology, Cambridge, MA, 2001.
[26] ABAQUS/CAE Version 6.11, Abaqus User Documentations, Dassault Systems, 2011.
[27] W. Hu, K.K. Choi, O. Zhupanska and J.H.J. Buchholz, A New Fatigue Analysis Procedure for Composite Wind Turbine Blades, *32nd ASME Wind Energy Symposium*, National Harbor, Maryland, 2014.
[28] Y. Liu and S. Mahadevan, Probabilistic fatigue life prediction of multidirectional composite laminates, *Composite Structures*, 69 (1), 11-19, 2005.
[29] R.V. Hoog, J.W. McKean and A.T. Craig, *Introduction to Mathematical Statistics, 6th Ed.*, Pearso Prentice Hall, Upper Saddle River, NJ, 2005.
[30] Y. Noh, K.K. Choi and I. Lee, Identification of marginal and joint CDFs using Bayesian method for RBDO,

Structural and Multidisciplinary Optimization, 40 (1), 35-51, 2010.
[31] TPI Composites Inc., Innovative Design Approaches for Large Wind Turbine Blades, Sandia Report SAND2003-0723, 2003.
[32] L. Zhao, K.K. Choi, I. Lee, Metamodeling Method Using Dynamic Kriging for Design Optimization, *AIAA Journal*, 49 (9), 2034-2046, 2011.
[33] I. Lee, K.K. Choi, Y. Noh, L. Zhao and D. Gorsich, Sampling-Based Stochastic Sensitivity Analysis using Score Functions for RBDO Problems with Correlated Random Variables, *Journal of Mechanical Design*, 133 (2), 021003, 2011.